2009

Error Control in Wireless Sensor Networks: A Cross Layer Analysis

Mehmet C. Vuran
University of Nebraska–Lincoln, mcvuran@cse.unl.edu

Ian F. Akyildiz
Georgia Institute of Technology

Error Control in Wireless Sensor Networks: A Cross Layer Analysis

Mehmet C. Vuran, *Member, IEEE*, and Ian F. Akyildiz, *Fellow, IEEE*

Abstract—Error control is of significant importance for Wireless Sensor Networks (WSNs) because of their severe energy constraints and the low power communication requirements. In this paper, a cross-layer methodology for the analysis of error control schemes in WSNs is presented such that the effects of multi-hop routing and the broadcast nature of the wireless channel are investigated. More specifically, the cross-layer effects of routing, medium access, and physical layers are considered. This analysis enables a comprehensive comparison of forward error correction (FEC) codes, automatic repeat request (ARQ), and hybrid ARQ schemes in WSNs. The validation results show that the developed framework closely follows simulation results.

Hybrid ARQ and FEC schemes improve the error resiliency of communication compared to ARQ. In a multi-hop network, this improvement can be exploited by constructing longer hops (*hop length extension*), which can be achieved through channel-aware routing protocols, or by reducing the transmit power (*transmit power control*). The results of our analysis reveal that for hybrid ARQ schemes and certain FEC codes, the hop length extension decreases both the energy consumption and the end-to-end latency subject to a target packet error rate (PER) compared to ARQ. This decrease in end-to-end latency is crucial for delay sensitive, real-time applications, where both hybrid ARQ and FEC codes are strong candidates. We also show that the advantages of FEC codes are even more pronounced as the network density increases. On the other hand, transmit power control results in significant savings in energy consumption at the cost of increased latency for certain FEC codes. The results of our analysis also indicate the cases where ARQ outperforms FEC codes for various end-to-end distance and target PER values.

Index Terms—Automatic repeat request, cross layer analysis, energy consumption, forward error correction, hybrid ARQ, latency, wireless sensor networks.

I. INTRODUCTION

WIRELESS sensor networks (WSNs) are characterized by collaborative information transmission from multiple sensor nodes observing a physical phenomenon [1]. Severe energy constraints of battery-powered sensor nodes necessitate energy-efficient communication protocols in order to fulfill application objectives. Moreover, the low power communication constraints of sensor nodes exacerbate the effects of the wireless channel leading to error-prone links. In WSNs, correlation between sensors can be exploited in terms of aggregation, collaborative source coding, or correlation-based protocols. Since these techniques aim to reduce the redundancy in the traffic, the reliability of the filtered packets is important for energy efficiency. Hence, energy efficient error control is of extreme importance. Moreover, the strict energy consumption requirements, the multi-hop structure of the WSNs, and the broadcast nature of the wireless channel necessitate a cross-layer investigation of the effects of error control schemes.

In this paper, a cross-layer analysis of error control schemes is presented. More specifically, the effects of multi-hop routing and the broadcast nature of the wireless communication are investigated to derive the equations governing the energy consumption, latency, and packet error rate (PER) performance of error control schemes. As a result, a cross layer analysis framework, which considers routing, medium access control, and physical layers, is devised. More specifically, we consider channel-aware geographical routing and contention-based MAC protocols. This analysis enables a comprehensive comparison of forward error correction (FEC), automatic repeat request (ARQ), as well as hybrid ARQ schemes in WSNs. In this paper, we have extended our work in [23], which is, to the best of our knowledge, the first work that considers both the broadcast wireless channel and the multi-hop structure of WSNs with realistic channel models and a two-dimensional topology. The investigation of Reed–Solomon codes has been included to provide a complete analysis of FEC codes in WSNs. Moreover, the effects of medium access control (MAC) has been incorporated into our framework. Furthermore, the advantages of hybrid ARQ schemes are explored. The developed framework is validated through simulation results and provides a practical comparison of these schemes by considering two major hardware architectures for WSNs, i.e., Mica2 [9] and MicaZ [10] nodes. It should be emphasized that in this work, we do not propose a new FEC code for WSNs. Rather, we devise a framework to assess the performance of FEC, ARQ, and hybrid ARQ schemes. Furthermore, our goal is to indicate the situations where one of the error control schemes should be favored.

The rest of this paper is organized as follows. In Section II, an overview of analysis on error control schemes in WSNs is provided. Our approach and the system model for cross-layer analysis are explained in Section III. In Section IV, the cross-layer analysis of ARQ, FEC, and hybrid ARQ schemes is presented. The numerical evaluations are explained in Section V along with their implications on the tradeoffs of error control schemes. Finally, the paper is concluded in Section VI.

II. RELATED WORK

Although there have been several studies on error control techniques in wireless networks and especially in cellular networks, none of them are directly applicable to WSNs. Especially, the limited energy consumption requirements and the low complexity in the sensor hardware necessitate energy efficient error control and prevent high complexity codes to be deployed. Recently, there have been some work that considers the energy consumption analysis of error control techniques in WSNs.

In [20], the energy consumption profile of convolutional codes has been presented based on a specific sensor node architecture, i.e., μAMPS node. It has been shown that convolutional codes results in lower energy efficiency compared to uncoded transmission for probability of bit error, $P_b > 10^{-5}$ [20]. Similarly, in [15], the energy efficiency of convolutional codes is compared to the energy efficiency of BCH codes in a framework to optimize the packet size in WSNs. The results of this work reveal that BCH codes outperform the most energy efficient convolutional code by almost %15. A similar result is reported in [4], where convolutional codes are shown to be inferior to block codes in terms of energy consumption. Consequently, we do not consider convolutional codes in our work due to their energy inefficiency. Although important insight on error control schemes in WSN has been provided in these work, still a point-to-point analysis has been conducted, which does not capture the cross-layer effects of medium access and multi-hop communication in WSNs.

Recently, rateless codes (LT- and Raptor codes) have been proposed that perform very close to the theoretical limit [14] and [19]. However, for these codes to perform efficiently, very long payload lengths of $k \sim 100\,000$ are required. Since the wireless sensor network hardware cannot support packet sizes larger than 120–250 bytes, rateless codes are not considered in our analysis.

In [17], an analysis of different modulation schemes and two BCH codes is presented based on their energy consumption efficiency. However, in this analysis, the energy consumption for transmitting redundant bits is considered as the only overhead of error control coding without considering the decoding energy. Similarly, in [4], the bit error rate (BER) performance and power consumption of block and convolutional codes are investigated considering a Gaussian channel. In both of these work, a single-hop WSN link is considered, which decouples multi-hop routing and the effects of error control codes.

In [11], the effect of error control coding on the energy consumption of multihop WSNs is studied. However, this analysis considers a linear topology, where the distances between each hop are fixed and equal. Moreover, for each link, the probability of error is assumed to be the same. Consequently, the fading effects of the wireless channel and the random route construction cannot be captured with the presented framework in [11]. Furthermore, the end-to-end latency has never been considered in the context of FEC codes in WSNs before.

Contrary to the existing work, we provide a cross-layer analysis of error control schemes in WSNs. More specifically, a cross layer analysis framework, which considers routing, medium access control, and physical layers, is devised. This is, to the best of our knowledge, the first work that considers the broadcast wireless channel and the multi-hop structure

of WSNs with realistic channel models and a 2 dimensional topology for error control analysis.

III. MOTIVATION AND SYSTEM MODEL

In general, the error control mechanisms can be categorized into three main approaches; automatic repeat request (ARQ), forward error correction (FEC), and hybrid ARQ as follows:

- *Automatic Repeat Request (ARQ)*: ARQ-based error control mainly depends on the retransmission for the recovery of the lost data packets. ARQ protocols enable retransmissions of failed packets by sending explicit acknowledgements upon failure. It is clear that ARQ error control mechanisms incur significant additional retransmission cost and overhead in case of errors. On the other hand, in the case of good channel quality, overhead of the ARQ protocols is low compared to FEC schemes. The efficiency of ARQ in sensor network applications is limited due to the scarcity of the energy and processing resources of the sensor nodes.

- *Forward Error Correction (FEC)*: FEC adds redundancy to the transmitted packet such that it can be received at the receiver error-free even if the limited number of bits are received in error. Consequently, FEC codes incur communication overhead in terms of transmission and reception of additional redundant bits as well as decoding packets. In WSNs, where low clock-rate CPUs are used, decoding energy should also be considered in assessing the performance of FEC protocols. There exist various FEC codes that are optimized for specific packet sizes, channel conditions, and reliability requirements such as linear block codes (BCH and Reed–Solomon (RS) codes) as well as convolutional codes. In our analysis, we consider BCH and RS codes because of their energy efficiency.

- *Hybrid ARQ (HARQ)*: Hybrid ARQ schemes aim to exploit the advantages of both FEC and ARQ schemes by incrementally increasing the error resiliency of a packet through retransmissions. Mainly, two types of HARQ schemes exist: Type I and Type II. With HARQ-I techniques, first an uncoded packet or a packet coded with a lower error correction capability is sent. If this packet is received in error, the receiver sends a negative acknowledgement (NACK) to the sender, which re-sends the packet coded with a more powerful FEC code. The difference in Type II is that for retransmissions, only the redundant bits are sent. While Type II decreases the bandwidth usage of the protocol, Type I does not require the previously sent packets be stored.

Forward error correction (FEC) coding and hybrid ARQ schemes improve the error resiliency compared to ARQ schemes by sending redundant bits through the wireless channel. Therefore, lower signal to noise ratio (SNR) values can be supported to achieve the same error rate as an uncoded transmission. This advantage can be exploited in two ways in WSNs to overcome the overhead because of increased communication and computation cost:

- *Hop Length Extension:* In multi-hop networks, the error resiliency of FEC and HARQ schemes can be exploited to improve the effective transmission range of a node. This is illustrated in Fig. 1, where the packet error rate contours
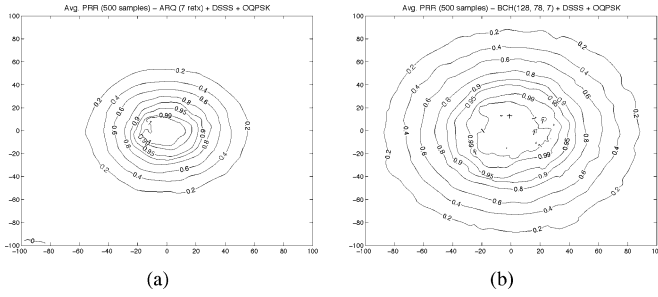
Fig. 1. 2-D average packet reception rate graphs for (a) ARQ ($N = 7$) and (b) FEC (BCH(128,78,7)) for MicaZ.

Fig. 2. Reference model for the derivations.

of ARQ and FEC codes are shown at around a transmitter node for a packet of 38 bytes for MicaZ nodes. Comparing Fig. 1(a) and (b), for a target packet reception rate of 0.9, the average transmission range of a node is 29 m for ARQ and 42 m for FEC with transmit power of -5 dBm. This clearly illustrates that FEC codes can increase the effective transmission range of a node compared to ARQ by using the same transmit power. This can be exploited to construct longer hops in a multi-hop network such as WSNs. We refer to this technique as *hop length extension*, which can be achieved through channel-aware cross-layer routing protocols as we will explain in the following sections.

- *Transmit Power Control:* The improved error resiliency provided through FEC codes can also be exploited by reducing the transmit power. This technique, which we refer to as *transmit power control*, improves the capacity of the network by reducing the interference to other users.

In the following, we investigate the tradeoffs between ARQ, FEC, and hybrid ARQ schemes in terms of energy consumption, latency, and end-to-end packet error rate considering the hop length extension and the transmit power control techniques to exploit the error resiliency of FEC and hybrid ARQ techniques. In our analysis, we consider a network composed of sensor nodes that are distributed according to a 2-D Poisson distribution with density ρ. Duty cycle operation is deployed such that each node is active for δ fraction of the time and is in sleep mode otherwise [2]. Moreover, we consider a monitoring application such that the reporting rates of sensors are low but the messages should be transmitted reliably subject to a certain end-to-end packet error rate target.

In order to realize hop length extension, we consider a channel-aware routing algorithm, where the next hop is determined according to the received signal-to-noise-ratio (SNR) of a packet sent from a specific node i at a distance D from the sink. Among the neighbors of i, the neighbor, j, that is closest to the sink and with SNR value, $\psi_j > \psi_{\text{Th}}$ is selected as the next hop, where ψ_{Th} is the received SNR threshold. This approach can be implemented using a cross-layer approach as in [2] or through signaling [18]. The medium access is performed through RTS-CTS-DATA exchange in addition to ACK and retransmissions for ARQ and NACK and retransmissions for hybrid ARQ.

Accordingly, first, the expected hop distance is derived as a function of the network parameters. Then, the end-to-end energy consumption, latency, and packet error rate (PER) of a single flow are derived. We use the model shown in Fig. 2 and the
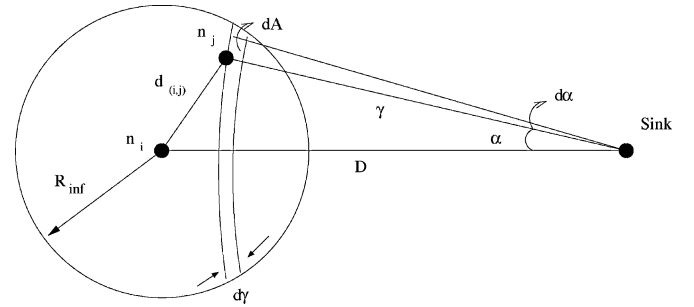
log-normal shadow fading channel model [26] for our derivations. Note that in such a model, the transmission range of a node is essentially infinite due to the shadow fading component. In our analysis, we approximate the transmission range of a node to R_{inf}, which is the distance at which the probability that a packet can be successfully received is negligible. Moreover, the distribution of hop distance and the associated parameters at each hop is considered independent since duty cycle operation is performed. As a result, the state of the network will change at each hop since different nodes will be awake at different time instants. In [22], duty cycle operation is not considered and hence, a different approach has been taken. Note that energy consumption analysis has been performed in a node-centric manner for routing algorithms in [21], [25]. However, these models do not incorporate the effects of neighbor nodes, the wireless channel quality, or the channel-aware routing decisions in this context. Moreover, the effects of channel conditions have not been taken into account in the derivations in [21], [25]. In our analysis, we investigate the energy consumption to transmit a packet to the sink with the effect of neighbor nodes and wireless channel effects, which provides a clear insight into the overall energy consumption in multi-hop WSNs.

Our cross-layer analysis framework enables comprehensive comparison of ARQ, FEC, and hybrid ARQ schemes. To illustrate specific results, we consider a block code, which is represented by (n, k, t), where n is the block length, k is the payload length, and t is the error correction capability in bits. More specifically, a block code of (n, k, t) can correct bit errors of up to t bits in a block of k information bits by sending n-k redundant bits. In our analysis, we use a series of extended BCH (n, k, t) codes with $n = 128$ and $t = \{2, 3, 5, 7, 9, 13, 21\}$, which enable the evaluation of the effect of error correction capability, t. Furthermore, we use the (7, 3, 2), (15, 9, 3), and (31, 19, 6) RS codes.[1] For the hybrid ARQ schemes, we consider three different configurations. For type-I hybrid ARQ (HARQ-I), we consider the case where first, an uncoded packet is sent followed by a packet encoded by BCH codes. Furthermore, a combination of two BCH codes is also considered for the HARQ-I. The type-II hybrid ARQ (HARQ-II) schemes require incremental error control coding since only the difference in redundant bits is sent through retransmissions. This is generally accomplished through punctured codes [24]. Since this procedure is energy consuming, we consider the case where the packet is encoded by a BCH code and then the payload is

---

[1]Note that other FEC schemes can also be used in our framework.

sent first. The receiver uses only the CRC bits in the payload for decoding. In case of errors, the receiver sends a NACK packet and the transmitter sends the redundant bits for BCH decoding. We consider only one retransmission is performed for the hybrid ARQ schemes. Throughout the paper, the hybrid ARQ schemes are indicated by a tuple (t_1, t_2), where the first parameter, t_1 indicates the error correction capability of the first packet and t_2 is that of the second packet. As an example, HARQ-II $(0, 3)$ refers to type-II hybrid ARQ, where first an uncoded packet is sent, i.e., $t_1 = 0$, and in case of channel errors, the redundant bits of the BCH (128, 106, 3) encoded packet is sent.

IV. CROSS-LAYER ANALYSIS

In this section, we first derive the expected hop distance by considering the effects of broadcast channel, medium access control, and channel-aware routing as discussed in Section III. The results of this analysis are validated through simulations and used to analyze the end-to-end energy consumption, latency, and packet error rate (PER) of FEC, ARQ, and hybrid ARQ schemes. First, we define the total energy consumed as a result of a single flow from a source node at distance D from the sink as follows:

$$E_{\text{flow}}(D) = \mathrm{E}[E_h]\,\mathrm{E}[n_h(D)] \qquad (1)$$

where $\mathrm{E}[E_h]$ is the expected energy consumption per hop and $\mathrm{E}[n_h(D)]$ is the expected hop count from a source at distance D to the sink. Similarly, the end-to-end latency of a flow is given by

$$T_{\text{flow}}(D) = \mathrm{E}[T_h]\,\mathrm{E}[n_h(D)] \qquad (2)$$

where $\mathrm{E}[T_h]$ is the expected delay per hop.

A good approximation for the expected hop count is given in [25] as

$$\mathrm{E}[n_h(D)] \simeq \frac{D - R_{\text{inf}}}{\mathrm{E}[d_h]} + 1 \qquad (3)$$

where D is the end-to-end distance, R_{inf} is the approximated transmission range, and $\mathrm{E}[d_h]$ is the expected hop distance. In Sections IV.A, IV.B, and IV.C, we derive the expressions for the expected hop length, $\mathrm{E}[d_h]$, the expected energy consumption per hop, $\mathrm{E}[E_h]$, and the expected latency per hop, $\mathrm{E}[T_h]$, respectively.

A. The Expected Hop Distance

Consider a node j in the infinitesimal area $dA = d\gamma d\alpha$ at coordinates (γ, α) with respect to the sink as shown in Fig. 2. The distance from node j to node i is, hence, given by

$$d_{(i,j)} = d(D, \gamma, \alpha) = \sqrt{\gamma^2 + D^2 - 2\gamma D \cos\alpha}. \qquad (4)$$

The expected hop distance, $\mathrm{E}[d_h]$, can be found as

$$\mathrm{E}[d_h] = \int_{\gamma_{\min}}^{D} \int_{-\alpha_\gamma}^{\alpha_\gamma} d_{(i,j)}\, d\mathrm{P}\{\mathcal{N}_i = j\} \qquad (5)$$

where $\gamma_{\min} = D - R_{\text{inf}}, d_{(i,j)}$ is the distance between nodes i and j as given by (4), $d\mathrm{P}\{\mathcal{N}_i = j\}$ is the probability that the next hop $\mathcal{N}_i$ is selected as node j, and $\alpha_\gamma = \mathrm{acos}[(\gamma^2 + D^2 - R_{\text{inf}}^2)/(2\gamma D)]$.

In order for node j to be selected as the next hop, first, the received SNR, ψ_k, at each node, k, which is closer to the sink than node j, should be lower than the SNR threshold, i.e., $\psi_k \leq \psi_{\text{Th}}$. Moreover, the received SNR of node j should satisfy, $\psi_j > \psi_{\text{Th}}$. Consequently, the probability that node j is selected as the next hop is given by

$$d\mathrm{P}\{\mathcal{N}_i = j\} = \mathrm{P}\{N_{A(d\gamma)} = 1\}\mathrm{P}\{\psi_j > \psi_{\text{Th}}\}\mathrm{P}\{d_{(j,s)} \geq \gamma\} \qquad (6)$$

where $N_{A(d\gamma)}$ is the number of nodes in the area, dA, at distance γ from the sink. The first component in (6) denotes the probability that there is a node inside the area $A(d\gamma)$. The second component, $\mathrm{P}\{\psi_j > \psi_{\text{Th}}\}$, in (6) is the probability that the received SNR of the node j is above ψ_{Th}. Finally, the third component, $\mathrm{P}\{d_{(j,s)} \geq \gamma\}$, is the probability that the next hop j is at least at a distance γ from the sink, s. By integrating through the feasible area as indicated by the limits in the integrals in (5), the expected hop distance can be found.

The first component, $\mathrm{P}\{N_{A(d\gamma)} = 1\}$, in (6) can be approximated by

$$\mathrm{P}\{N_{A(d\gamma)} = 1\} \simeq 1 - e^{-\rho\delta\gamma d\gamma d\alpha} \text{ as } d\gamma \to 0$$
$$\simeq \rho\delta\gamma d\gamma d\alpha \qquad (7)$$

where we use the approximation $e^{-x} \simeq 1 - x$ for the last step since $(\rho\delta\gamma d\gamma d\alpha) \to 0$ as $d\gamma \to 0, d\alpha \to 0$.

For the calculation of $\mathrm{P}\{\psi_j > \psi_{\text{Th}}\}$ and $\mathrm{P}\{d_{(j,s)} \geq \gamma\}$ in (6), we first introduce the log-normal channel model [26], where the received power at a receiver at distance d from a transmitter is given by

$$P_r(d) = P_t - \mathrm{PL}(d_0) - 10\eta\log_{10}\left(\frac{d}{d_0}\right) + X_\sigma \qquad (8)$$

where P_t is the transmit power in dBm, $\mathrm{PL}(d_0)$ is the path loss at a reference distance d_0 in dB, η is the path loss exponent, and X_σ is the shadow fading component, with $X_\sigma \sim \mathcal{N}(0, \sigma)$. Moreover, the signal to noise ratio (SNR) at the receiver is given by $\psi(d) = P_r(d) - P_n$ in dB, where P_n is the noise power in dBm.

Considering the shadow fading component, X_σ, the second term in (5), i.e., the probability that ψ_j is above SNR threshold, ψ_{Th}, is

$$\mathrm{P}\{\psi_j > \psi_{\text{Th}}\} = \mathrm{P}\{X_\sigma > \beta(d_{(i,j)}, \psi_{\text{Th}})\}$$
$$= Q\left(\frac{\beta(d_{(i,j)}, \psi_{\text{Th}})}{\sigma}\right) \qquad (9)$$

where

$$\beta(d_{(i,j)}, \psi_{\text{Th}}) = \psi_{\text{Th}} + P_n - P_t + \mathrm{PL}(d_0) + 10\eta\log_{10}\left(\frac{d_{(i,j)}}{d_0}\right) \qquad (10)$$

and $Q(x) = 1/\sqrt{2\pi}(\int_x^\infty e^{-(t^2/2)})dt$.

According to the channel model above, by denoting the area that consists of nodes that are closer to the sink than node j as $A(\gamma)$, $\mathrm{P}\{d_{(j,s)} \geq \gamma\}$ can be found as

$$\mathrm{P}\left\{d_{(j,s)} \geq \gamma\right\} = \sum_{i=0}^{\infty} \mathrm{P}\left\{N_{A(\gamma)} = i\right\} p_k(\gamma)^i$$
$$= \sum_{i=0}^{\infty} \frac{e^{-M(\gamma)} M(\gamma)^i}{i!} p_k(\gamma)^i$$
$$= e^{-M(\gamma)(1-p_k(\gamma))} \qquad (11)$$

where $A(\gamma)$ is the area of intersection of two circles with centers separated by D and with radii $R_{\inf}$ and γ, respectively. Consequently, $N_{A(\gamma)}$ is the number of nodes in $A(\gamma)$ and $M(\gamma) = \rho\delta A(\gamma)$ is the average number of nodes in this area. Moreover, $p_k(\gamma) = \mathrm{P}\{\psi_k \leq \psi_{\mathrm{Th}}, k \in A(\gamma)\}$ is the probability that for a node k in $A(\gamma)$, the received SNR is less than the SNR threshold, i.e., $\psi_k \leq \psi_{\mathrm{Th}}$. This can found as

$$p_k(\gamma) = \int_{\gamma_{\min}}^{\gamma} \int_{-\alpha_\gamma}^{\alpha_\gamma} \left[1 - Q\left(\frac{\beta}{\sigma}\right)\right] \frac{1}{A(\gamma)} d\alpha d\gamma \qquad (12)$$

where $\gamma_{\min} = D - R_{\inf}$.

Using (6), (7), (9), (11), and (12) in (5), the expected hop distance can be calculated as follows:

$$\mathrm{E}[d_h] = \rho\delta \int_{\gamma_{\min}}^{D} \int_{-\alpha_\gamma}^{\alpha_\gamma} \gamma d_{(i,j)} Q\left(\frac{\beta}{\sigma}\right) e^{-M(\gamma)(1-p_k(\gamma))} d\alpha\, d\gamma \qquad (13)$$

which will be used for energy consumption and latency analysis of FEC, ARQ, and hybrid ARQ schemes according to (1), (2), and (3).

B. Energy Consumption Analysis

The expected energy consumption and latency per hop are also calculated by considering a node j as shown in Fig. 2. We denote the expected energy consumption between node i and node j by $\mathrm{E}[E_j]$, which is a function of γ and α. Following the same derivations in Section IV.A and replacing $d_{(i,j)}$ by $\mathrm{E}[E_j]$ in (13), the expected energy consumption per hop is found as

$$\mathrm{E}[E_h] = \rho\delta \int_{\gamma_{\min}}^{D} \int_{-\alpha_\gamma}^{\alpha_\gamma} \gamma \mathrm{E}[E_j] Q\left(\frac{\beta}{\sigma}\right) e^{-M(\gamma)(1-p_k(\gamma))} d\alpha\, d\gamma. \qquad (14)$$

Since a node can become a next hop if its received SNR value is above a certain threshold, the expected energy consumption, $\mathrm{E}[E_j]$, in (14) can be found as

$$\mathrm{E}[E_j] = \int_{\psi_{\mathrm{Th}}}^{\infty} E_{\mathrm{comm}}(d_{(i,j)}, \psi) f_\Psi(d_{(i,j)}, \psi) d\psi \qquad (15)$$

where $E_{\mathrm{comm}}(d_{(i,j)}, \psi)$ is the energy consumption for communication between nodes i and j given that they are at a distance $d_{(i,j)}$ and the SNR value at node j is ψ. Moreover, $f_\Psi(\cdot)$ is the pdf of the SNR, which is a function of $d_{(i,j)}$ as well. Since $P(\Psi \leq \psi) = P(X_\sigma \leq \beta(d_{(i,j)}, \psi))$, $f_\Psi(\cdot)$ is found as

$$f_\Psi(d_{(i,j)}, \psi) = f_{X_\sigma}\left(\beta(d_{(i,j)}, \psi)\right)$$
$$= \frac{1}{\sigma\sqrt{2\pi}} e^{-\left(\beta(d_{(i,j)}, \psi)\right)^2/2\sigma^2} \qquad (16)$$

where $\beta(d_{(i,j)}, \psi)$ is given in (10).

The first component, $E_{\mathrm{comm}}(d_{(i,j)}, \psi)$, in (15) is the energy consumption to transmit a packet between two nodes at a distance $d_{(i,j)}$ with received SNR ψ and has three components as given by[2]

$$E_{\mathrm{comm}} = E_{TX} + E_{RX} + E_{\mathrm{neigh}} \qquad (17)$$

where E_{TX} is the energy consumed by the node transmitting the packet (node i), E_{RX} is the energy consumed by the node receiving the packet (node j), and E_{neigh} is the energy consumed by the neighbor nodes.

In order to successfully transmit the packet, a node needs to complete the four-way RTS-CTS-DATA-ACK handshake for ARQ, three-way RTS-CTS-DATA handshake for FEC codes, and RTS-CTS-DATA-NACK exchange for hybrid ARQ. Before transmitting an RTS packet, for medium access, we assume that a node performs carrier sense mechanism to assess the availability of the channel and transmits a packet thereafter. Note that if a reservation-based protocol is used, collisions may be neglected. In those cases, the remainder of our framework still applies [23]. Many work focus on the investigation of medium access performance of carrier sense mechanisms [5], [7], [8], [17]. Without loss of generality, here, we refer to the work in [17]. Note that our contribution is not to produce yet another analysis of carrier sense mechanism. Rather, we aim to illustrate the impact of MAC on error control in WSNs.

A successful allocation of the channel depends on both successful carrier sense and the fact that the transmission encounters no collisions. The probability of successful carrier sense, p_{cs}, can be denoted as follows [17]:

$$p_{\mathrm{cs}} = 1 - (1 - p_{\mathrm{cf}})^{K+1} \qquad (18)$$

where K is the number of re-sensings allowed for one transmission and p_{cf} is the probability of sensing the channel free, which is given by:

$$p_{\mathrm{cf}} = e^{-\lambda_{\mathrm{net}}(\tau_{\mathrm{cs}} + T_{\mathrm{comm}})} \qquad (19)$$

where τ_{cs} is the carrier sense period and T_{comm} is the duration of a packet transmission. After a successful carrier sense, a collision can only occur if another node transmits during the vulnerable period of τ_{cs}. As a result, the probability of no collisions, p_{noColl}, is given by

$$p_{\mathrm{noColl}} = e^{-\lambda_{\mathrm{net}}\tau_{\mathrm{cs}}} \qquad (20)$$

The term λ_{net} that appears in both (19) and (20) refers to the overall traffic that is generated by all the nodes inside the transmission range of a node, which is given by

$$\lambda_{\mathrm{net}} = \lambda \frac{p_{\mathrm{cs}}}{p_{\mathrm{comm}}} (1 - (1 - p_{\mathrm{comm}})^{L+1}) \qquad (21)$$

where λ is the total generated traffic in the transmission range of a node and p_{comm} is the probability of successful transmission. Accordingly, the probability that a node can successfully acquire the channel is given by $p_{\mathrm{cs}} p_{\mathrm{noColl}}$, which can be found by solving the system of (18), (20)–(21).

---

[2]We drop the indices ψ and $d_{(i,j)}$ for ease of illustration.

The total generated packet rate, λ, depends on both the generated traffic rate and the size of the packet. Let us assume that the sensor node has an average sampling rate of b bits/s. Denoting the length of the packet payload as l_D, on the average, the packet generation rate of a node i is $\lambda_{ii} = b/l_D$ pkts/s. Since a node will also relay packets from other nodes to the sink, the packet transmission rate of a node is higher than this value. If a routing scheme that equally shares the network load among nodes is considered, on the average, the packet transmission rate of a node is $\lambda_i = c_i \lambda_{ii}$, where $c_i > 1$. Consequently, λ in (21) is given by $\lambda = \sum_{i=1}^{M_n} \lambda_i$, where the number of nodes that are in the transmission range of a node is given by $M_n - 1$.

Upon accessing the channel, the energy consumption depends on the probability that a data and a control packet is successfully received at distance $d_{(i,j)}$ with SNR, ψ, which are denoted as $p_s^D(\psi)$ and $p_s^C(\psi)$, respectively.[3] The derivations of $p_s^D(\psi)$ and $p_s^C(\psi)$ are explained in Section IV.E. In addition, an RTS packet transmission is only successful if a node can successfully acquire the channel (given by $p_{cs}p_{noColl}$). Accordingly, E_{TX} is given in (24), (25), and (26) for ARQ, FEC, and HARQ, respectively, where

$$n_{ret}^{ARQ} = \left(1 - p_{cs} + p_{cs}p_{noColl}\left(p_s^C\right)^3 p_s^D\right)^{-1}, \quad (22)$$

$$n_{ret}^{FEC} = n_{ret}^{HARQ} = \left(1 - p_{cs} + p_{cs}p_{coll}\left(p_s^C\right)^2\right)^{-1} \quad (23)$$

are the expected number of retransmissions for ARQ, FEC, and HARQ, which are further limited by the allowed maximum number of retransmissions.

$$\begin{aligned} E_{TX}^{ARQ} &= n_{ret}^{ARQ} \{E_{sense} \\ &+ p_{cs}\left(E_{tx}^C + p_{noColl}p_s^C E_{rx}^C + p_{noColl}\left(p_s^C\right)^2 E_{tx}^D\right. \\ &+ p_{noColl}\left(p_s^C\right)^2 p_s^D E_{rx}^C \\ &+ \left(1 - p_{noColl}p_s^C\right)E_{t/o}^C \\ &+ \left. p_{noColl}\left(p_s^C\right)^2\left(1 - p_s^D\right)E_{t/o}^D\right)\}, \quad (24) \end{aligned}$$

$$\begin{aligned} E_{TX}^{FEC} &= n_{ret}^{FEC}\{E_{sense} + p_{cs}\left(E_{tx}^C + p_{coll}p_s^C\left(E_{rx}^C + E_{dec}^C\right)\right. \\ &+ \left.\left(1 - p_{coll}p_s^C\right)E_{t/o}^C\right)\} + p_{cs}p_{coll}\left(p_s^C\right)^2 E_{tx}^D, \quad (25) \end{aligned}$$

$$\begin{aligned} E_{TX}^{HARQ} &= n_{ret}^{HARQ}\{E_{sense} + p_{cs}\left(E_{tx}^R + E_{rx}^C + E_{dec}^C + E_{tx}^{D1}\right)\} \\ &+ \left(p_s^C\right)^2\left(1 - p_s^{D1}\right)\left(E_{rx}^N + E_{dec}^C + E_{tx}^{D2}\right). \quad (26) \end{aligned}$$

In (24), (25), and (26), E_{tx}^x and E_{rx}^x are the packet transmission and receiving energies for packets, where the superscripts R, C, D, and A refer to RTS, CTS, DATA, and ACK packets, respectively. The first term in (24) is the expected number of retransmissions, which is a function of probability of successful carrier sense, p_{cs}, the probability of no collisions, p_{noColl}, and the successful transmission probability of control and data packets. The first term in parenthesis, E_{sense}, is the energy

[3]We consider the length of RTS, CTS, ACK, and NACK packets the same and drop the indices ψ in the remaining for clarity.

consumption for sensing the region. If the channel sensing is successful, the node transmits an RTS packet and receives a CTS packet if there is no collision and the RTS packet is successfully received at the destination. Similarly, data packet is sent if the CTS packet is received successfully, followed by an ACK packet reception. The last two terms in the parentheses are the energy consumption for the timeout for CTS and ACK packets in case of packet errors. Similarly, E_{TX} for FEC and hybrid ARQ can be found as in (25), and (26), respectively, where E_{dec}^x is the decoding energy and the subscripts $D1$ and $D2$ in (26) refer to the transmitted packets for the first and second transmission in hybrid ARQ. In our calculations, we assume that RTS and CTS packets are also encoded in order to fully exploit the advantages of FEC codes. Using the same approach, the energy consumption of the receiver node, E_{RX} in (17), is given as follows:

$$E_{RX}^{ARQ} = n_{ret}^{ARQ}\left\{E_{rx}^R + E_{tx}^C + E_{rx}^D + E_{tx}^A\right\}, \quad (27)$$

$$E_{RX}^{FEC} = n_{ret}^{FEC}\left\{E_{rx}^R + E_{dec}^R + E_{tx}^C + E_{rx}^D + E_{dec}^D\right\}, \quad (28)$$

$$\begin{aligned} E_{RX}^{HARQ} &= n_{ret}^{HARQ}\left\{E_{rx}^R + E_{dec}^R + E_{tx}^C\right\} + E_{rx}^{D1} + E_{dec}^{D1} \\ &+ \left(p_s^C\right)^2\left(1 - p_s^{D1}\right)\left(E_{tx}^N + E_{rx}^{D2} + E_{dec}^{D2}\right), \quad (29) \end{aligned}$$

for ARQ, FEC, and hybrid ARQ, respectively.

The last term in (17), E_{neigh}, is the energy consumed by the neighbors of the transmitter and the receiver nodes, which is shown in (30) and (31) for ARQ, hybrid ARQ, and FEC codes:[4]

$$\begin{aligned} E_{neigh}^{ARQ} &= n_{ret}^{ARQ}\left\{\left(\rho\delta\pi R_{inf}^2 - 2\right)E_{rx}^R\right. \\ &+ \left.\left[\rho\delta\left(\pi R_{inf}^2 - A(D, R_{inf}, D)\right) - 2\right]E_{rx}^C\right\}, \quad (30) \end{aligned}$$

$$\begin{aligned} E_{neigh}^{FEC} &= E_{neigh}^{HARQ} = n_{ret}^{FEC}\left(\rho\delta\pi R_{inf}^2 - 2\right)E_{rx}^R \\ &+ \left[\rho\delta\left(\pi R_{inf}^2 - A(D, R_{inf}, D)\right) - 2\right]E_{rx}^C. \quad (31) \end{aligned}$$

Using these derivations in (1), the end-to-end energy consumption can be calculated for each error control technique.

C. Latency Analysis

The expression for end-to-end latency of a flow is derived using the similar approach above. The delay per hop is given by

$$\mathrm{E}[T_h] = \rho\delta\int_{\gamma_{min}}^{D}\int_{-\alpha_\gamma}^{\alpha_\gamma}\gamma\mathrm{E}[T_j]Q\left(\frac{\beta}{\sigma}\right)e^{-M(1-p_k)}d\alpha d\gamma \quad (32)$$

where

$$\mathrm{E}[T_j] = \int_{\psi_{Th}}^{\infty}T_{comm}(\psi, d_{(i,j)})f_\Psi(\psi, d_{(i,j)})d\psi \quad (33)$$

and T_{comm} is given in (34), (35), and (36) for ARQ, FEC, and hybrid ARQ, respectively, where T_{sense} is the time spent for sensing, T^{Ctrl} and T^D are the control and data packet transmission time, respectively, $T_{t/o}$ is the timeout value, and T_{dec}^{Ctrl} and

[4]We assume the header information is sufficient for backoff.

T_{dec}^D are the decoding latency for control and data packets, respectively. The derivations of (34), (35), and (36) follow a similar approach as in (24).

$$
\begin{aligned}
T_{\text{comm}}^{\text{ARQ}} &= n_{\text{ret}}^{\text{ARQ}} \Big\{ T_{\text{sense}} + 2 p_{\text{cs}} p_{\text{noColl}} \left(p_s^C\right)^2 T^{\text{Ctrl}} \\
&+ p_{\text{cs}} \left(1 - p_{\text{noColl}} \left(p_s^C\right)^2\right) T_{t/o}^C \\
&+ p_{\text{cs}} p_{\text{noColl}} \left(p_s^C\right)^3 p_s^D \left(T^D + T^{\text{Ctrl}}\right) \\
&+ p_{\text{cs}} p_{\text{noColl}} \left(p_s^C\right)^3 \left(1 - p_s^C p_s^D\right) T_{t/o}^A \Big\},
\end{aligned}
\tag{34}
$$

$$
\begin{aligned}
T_{\text{comm}}^{\text{FEC}} &= n_{\text{ret}}^{\text{FEC}} \Big\{ T_{\text{sense}} + 2 T^{\text{Ctrl}} + 2 T_{\text{dec}}^C + T^D + T_{\text{dec}}^D \Big\},
\end{aligned}
\tag{35}
$$

$$
\begin{aligned}
T_{\text{comm}}^{\text{HARQ}} &= n_{\text{ret}}^{\text{HARQ}} \Big\{ T_{\text{sense}} + 2 T^{\text{Ctrl}} + 2 T_{\text{dec}}^C + T^{D1} + T_{\text{dec}}^{D1} \Big\} \\
&+ \left(p_s^C\right)^2 \left(1 - p_s^{D1}\right) \left(T^{\text{Ctrl}} + T_{\text{dec}}^C + T^{D2} + T_{\text{dec}}^{D2}\right).
\end{aligned}
\tag{36}
$$

D. Decoding Latency and Energy

One of the major overheads of FEC codes in addition to transmission and reception of redundant bits is the energy consumption for encoding and decoding packets as well as the delay associated with it. It is well known that the encoding energy for block codes is negligible [13]. Hence, we only consider the decoding energy and latency in our calculations in Sections IV.B and IV.C. The Mica2 and MicaZ nodes that we consider for our analysis do not provide hardware support for FEC coding [9], [10]. Hence, we assume that FEC coding is implemented in software. According to [13], the latency of decoding for a block code (n, k, t) is given as

$$
T_{\text{dec}}^{BL} = (2nt + 2t^2)(T_{\text{add}} + T_{\text{mult}})
\tag{37}
$$

where T_{add} and T_{mult} are the latency for addition and multiplication, respectively, of field elements in $\text{GF}(2^m), m = \lfloor \log_2 n + 1 \rfloor$ [15]. Both Mica2 and MicaZ nodes are implemented with 8-bit microcontrollers [3], which can perform addition and multiplication of 8 bits in 1 and 2 cycles, respectively. As a result,

$$
T_{\text{add}} + T_{\text{mult}} = 3 \left\lceil \frac{m}{8} \right\rceil t_{\text{cycle}}
\tag{38}
$$

where t_{cycle} is one cycle duration, which is 250 ns for both Mica2 and MicaZ [3]. Consequently, the decoding energy consumption is $E_{\text{dec}}^{BL} = I_{\text{proc}} V T_{\text{dec}}^{BL}$, where I_{proc} is the current for processor, V is the supply voltage, and T_{dec}^{BL} is given in (37).

E. Bit and Packet Error Rate

In this section, we derive the expressions for bit and packet error rate for Mica2 and MicaZ nodes. Since the modulation schemes used in these nodes are significantly different, it is necessary to investigate the effects of FEC and hybrid ARQ on these nodes separately. Mica2 nodes are implemented with non-co-

herent FSK modulation scheme. The bit error rate of this scheme is given by [13]:

$$
p_b^{\text{FSK}} = \frac{1}{2} e^{-\frac{Eb/No}{2}}, \quad Eb/No = \psi \frac{B_N}{R}
\tag{39}
$$

where ψ is the received SNR, B_N is the noise bandwidth, and R is the data rate. The modulation scheme used in MicaZ nodes is offset quadrature phase shift keying (O-QPSK) with direct sequence spread spectrum (DSSS). The bit error rate of this scheme is given by [12]:

$$
p_b^{\text{OQPSK}} = Q(\sqrt{(Eb/No)_{\text{DS}}})
\tag{40}
$$

where

$$
(Eb/No)_{\text{DS}} = \frac{2N \times Eb/No}{N + 4\text{Eb}/\text{No}(K - 1)/3}
$$

where N is the number of chips per bit, and K is the number of simultaneously transmitting users.

Based on the bit error rate p_b, the PER for the error control schemes can be calculated as follows. For ARQ, the CRC-16 error detection mechanism is deployed in both Mica nodes. Assuming all possible errors in a packet can be detected, the PER of a single transmission of a packet with payload l bits is given by

$$
\text{PER}^{\text{CRC}}(l) = 1 - (1 - p_b)^l.
\tag{41}
$$

For the BCH codes, assuming perfect interleaving at the transceiver, the block error rate (BLER) is given by

$$
\text{BLER}(n, k, t) = \sum_{i=t+1}^{n} \binom{n}{i} p_b^i (1 - p_b)^{n-i}.
\tag{42}
$$

The block error rate for RS codes are found through simulations. More specifically, Berlekamp–Massey algorithm [6] is implemented and simulated to find the relationship between the block error rate and the bit error rate.

Since a packet can be larger than the block length n, especially where small block lengths are used, the PER for FEC is given by

$$
\text{PER}^{\text{FEC}}(l, n, k, t) = 1 - (1 - \text{BLER}(n, k, t))^{\lceil \frac{l}{k} \rceil}
\tag{43}
$$

where $\lceil \frac{l}{k} \rceil$ is the number of blocks required to send l bits and $\lceil \cdot \rceil$ is the ceiling function. Using (41), (42), and (43), the PER for the hybrid ARQ schemes are also found. The packet success probabilities p_s^C and p_s^D used in Section IV for control and data packets can then be found by using $l = l_C$ and $l = l_D$, respectively.

V. NUMERICAL RESULTS

In this section, we investigate the effects of FEC and hybrid ARQ schemes in terms of PER, energy consumption and end-to-end latency in a multi-hop network via numerical evaluations in MATLAB and simulations. The developed framework is validated through simulations and the cases where FEC and hybrid ARQ can be more favorable than ARQ are discussed. Moreover, an energy and latency-based taxonomy is devised to quali-
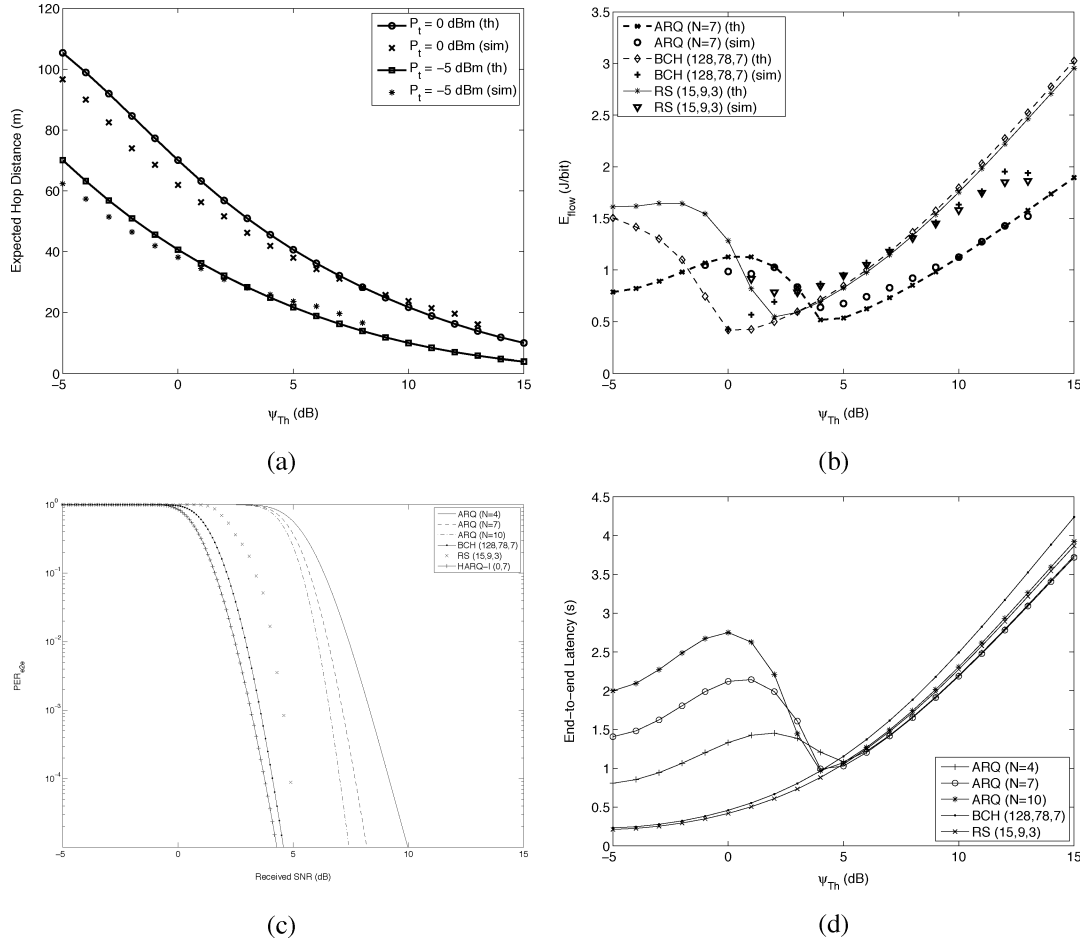
Fig. 3. (a) Average hop distance and (b) average energy consumption of a flow versus ψ_{Th}. (c) End-to-end PER versus ψ_{Th} and (d) average end-to-end latency versus ψ_{Th} (MicaZ).

TABLE I
PARAMETERS

D	300 m	l_C	8 bytes
P_t	0, -5, -15 dBm	l_D	38 bytes
PL_{d0}	55 dB	t_{cycle}	250 ns
P_n	-105 dBm	I_{proc}	8 mA
η	3	V	3 V
σ	3.8		
	Mica2		MicaZ
e_{rx}	21 mJ		59.1 mJ
e_{tx} (P_t=0)	24 mJ		52.2 mJ
e_{tx} (P_t=-5)	21.3 mJ		42 mJ
e_{tx} (P_t=-15)	16.2 mJ		29.7 mJ
$t_{bit} = 1/R$	62.4 μs		4 μs
N	N/A		16 chips
K	N/A		2

tatively compare FEC schemes with ARQ. For this comparison, two sensor node architectures are considered, i.e., Mica2 [9] and MicaZ [10]. We consider a multi-hop network, where a random access scheme and a channel-aware routing protocol is deployed as discussed in Section III. Unless otherwise noted, the parameters in Table I are used for the numerical results. For Mica2 nodes, the experimental values in [16] are used while for MicaZ, the values on the datasheet are used [10].

In addition to the numerical evaluations, simulations are also performed to validate the theoretical results. The simulation platform is developed in C++ [2], where a network of 300 nodes randomly deployed in a 300×300 area is considered. Packets generated from a node at the side of the network are sent to the sink on the other side of the network through channel-aware routing. The simulation results for average hop distance and the end-to-end energy consumption are shown in Fig. 3(a) and (b). Each result is an average of 5000 packet transmissions for each randomly generated topology, with five different topologies considered.

The expected hop distance d_{hop}, which is found in (5), is shown in Fig. 3(a) as a function of the received SNR threshold, ψ_{Th}, for different transmit power values, P_t. It can be observed that for small values of the received SNR threshold, ψ_{Th}, the average hop distance increases. Since lower ψ_{Th} allows nodes with lower channel quality to be chosen as the next hop, further nodes may become the next hop. Therefore, the number of hops from a node to a sink decreases for smaller ψ_{Th} values. Moreover, when the transmit power of a node is decreased, the expected hop distance decreases as expected. The simulation results are also shown in Fig. 3(a). Note that for high ψ_{Th} values, the simulation results are not shown since statistically valid results are not obtained because of the limited density in the network. For $\psi_{\mathrm{Th}} \leq 9$ dB, simulation results follow the theoretical results closely.

In the following, we present the effects of two techniques to exploit FEC codes in WSNs, i.e., hop length extension and transmit power control defined in Section III. First, two FEC schemes, BCH and RS codes, are compared with the ARQ scheme. Then, the effects of end-to-end distance, the end-to-end target PER, and the medium access control on the choice of error control scheme are also discussed. Furthermore, the results for hybrid ARQ are presented.

A. Hop Length Extension

In Fig. 3(b), the end-to-end energy consumption per useful bit is shown as a function of the SNR threshold, ψ_{Th}. The energy consumption is shown for ARQ with maximum number of retransmissions ($N = 7$), BCH (128,78,7) and RS (15,9,3) codes. The simulation results are also shown in Fig. 3(b). As shown in Fig. 3(b), the energy consumption of a flow decreases when ψ_{Th} value is decreased from 15 dB. This is mainly because of the increase in expected hop distance as shown in Fig. 3(a). However, the energy consumption for ARQ significantly increases as ψ_{Th} is decreased below a specific value, e.g., 5 dB. A lower ψ_{Th} results in nodes with lower channel quality to be selected as the next hop. As a result, retransmissions occur, which increase the energy consumption per hop. Although the expected number of hops decreases, the increase in energy consumption per hop dominates the total energy consumption for ARQ. Note that for ARQ, the energy consumption curve reaches a peak point and decreases as ψ_{Th} is decreased. This point corresponds to the case that the maximum number of retransmissions are no longer sufficient for reliable communication. The simulation results also reveal the accuracy of the proposed framework. For practical values of SNR threshold, ψ_{Th}, the simulation results closely follow the theoretical results.

When the FEC codes are considered, the energy consumption can be decreased at lower SNR threshold values. When ARQ and FEC codes are compared, for large ψ_{Th} values, ARQ clearly outperforms the FEC codes. However, BCH (128,78,7), and RS (15,9,3) codes are more energy efficient for smaller ψ_{Th} (~ 2 dB). The simulation results for each error control scheme are also shown in Fig. 3(b). It can be seen that the proposed framework closely follows the simulation results. Although this figure clearly shows the energy consumption of the two schemes as a function of ψ_{Th}, the operating points of ψ_{Th} for ARQ and FEC has to be determined. Moreover, the energy consumption because of lost packets are not captured through these figures. Hence, next, we investigate the end-to-end PER performance.

The PER for ARQ and FEC codes are given in (41) and (43), respectively. Since these equations show the PER for a single hop, here we extend these equations for the multi-hop case. Note that WSN applications are interested in the achievable end-to-end PER bound rather than the single hop PER. Hence, the relation between ψ_{Th} and the end-to-end PER bound can be used to determine the optimal point for ψ_{Th} in Fig. 3(b). Denoting the PER of a hop i by PER_i, there exists a π such that

$$\text{PER}_i \leq \pi, \quad \text{for } \psi_i \geq \psi_{\text{Th}},$$

where ψ_i is the received SNR at the hop i and $\pi = f(\psi_{\text{Th}})$, which can be calculated using (39)–(43) by replacing ψ with ψ_{Th} in (39). Since the end-to-end PER is

$$\text{PER}_{e2e} = 1 - \Pi_{i=1}^{n_h}(1 - \text{PER}_i)$$

where n_h is the number of hops, PER_{e2e} is bounded by

$$\text{PER}_{e2e} \leq 1 - (1 - \pi)^{n_h}, \text{ for } \psi_i \geq \psi_{\text{Th}}, \quad \forall\, i. \qquad (44)$$

Now assume that the end-to-end PER needs to be bounded by a certain threshold, PER_{e2e}^*, according to the application requirements. Accordingly, the route selection needs to be performed such that

$$\psi_{\text{Th}} = f^{-1}(1 - [1 - \text{PER}_{e2e}^*]^{1/n_h}). \qquad (45)$$

The relationship between the end-to-end PER, PER_{e2e}, and received SNR is shown in Fig. 3(c) for ARQ, BCH, RS, and hybrid ARQ schemes for MicaZ nodes. Note that for RS codes, the results of the simulations are used as explained in Section IV.E, whereas for ARQ, BCH, and HARQ, (41) and (43) are used. According to Fig. 3(c), the operating point for ψ_{Th} corresponding to a target end to end PER can be found. As an example, if the target PER of an application is 10^{-2}, the minimum value for ψ_{Th} corresponds to 6.1 dB for ARQ, 3 dB for BCH(128,78,7), 4.8 dB for RS(15,9,3), and 2.5 dB for HARQ-I. As a result, it can be observed from Fig. 3(b) that BCH (128,78,7) is slightly more energy efficient than ARQ. On the other hand, the RS (15,9,3) code results in higher energy consumption compared to the ARQ scheme. It is clear that more energy is consumed per hop for FEC codes due to both transmission of redundant bits and decoding. However, since the error resiliency is improved with FEC codes, lower SNR values can be supported. Through a channel-aware routing protocol that exploits this property, longer hop distances can be achieved leading to lower end-to-end energy consumption.

Exploiting FEC schemes with channel-aware routing not only improves energy consumption performance but the end-to-end latency can also be decreased significantly as shown in Fig. 3(d). It is clear that both FEC schemes outperform ARQ since their optimal ψ_{Th} value is lower than that of ARQ. This is due to both longer hops for FEC codes and the additional retransmissions of ARQ. Since the decoding delay of the FEC codes is lower than the time consumed for retransmission of a packet, FEC schemes improve the latency performance of the WSN. Furthermore, RS codes provide slightly lower end-to-end latency when compared to the BCH codes. This is related to the better error correction capability of RS codes when same number of redundant bits are sent. Consequently, the end-to-end latency is slightly decreased.

As shown in Fig. 3(b) and (d), energy consumption and latency are two main performance metrics for WSNs. In order to capture the efficiency of an error control scheme in terms of both of these parameters, we propose a taxonomy function that consists of the energy consumption, latency, and PER performance. This function is defined as follows:

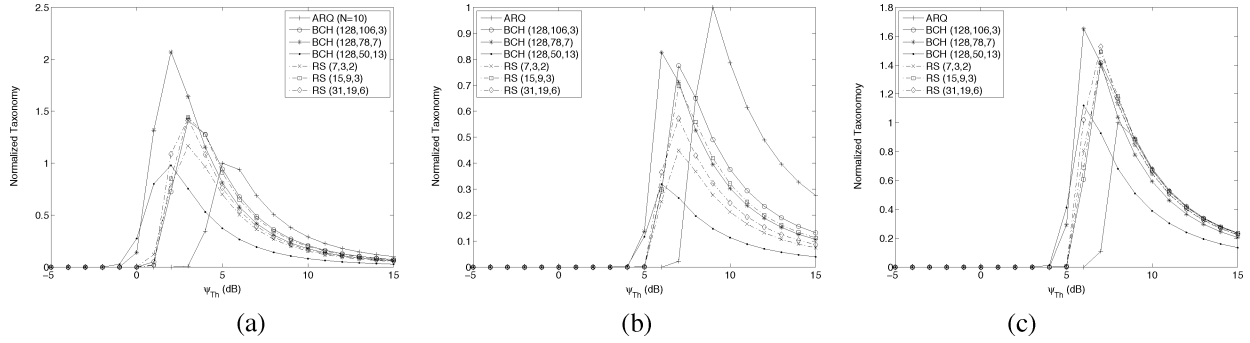$$\mathcal{T} = \frac{l_D}{E_{\text{flow}} T_{\text{flow}}}(1 - \text{PER}_{e2e}) \qquad (46)$$

Fig. 4. Taxonomy function versus ψ_{Th} for (a) MicaZ, (b) Mica2, and (c) Mica2 without E_{neigh}.
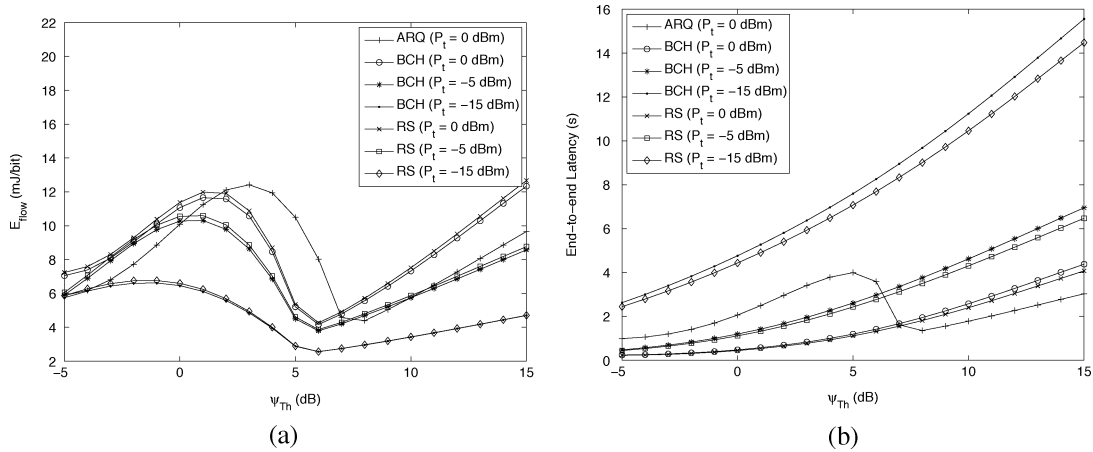

Fig. 5. (a) Average energy consumption of a flow and (b) average end-to-end latency versus ψ_{Th} for different values of transmit power (Mica2).

where l_D is the payload length, E_{flow}, T_{flow}, and PER_{e2e} are the end-to-end energy consumption, latency, and PER, respectively. Note that a similar efficiency function has been proposed in [15], where the energy efficiency and the reliability of a *single hop* has been considered. In our approach, we also consider the cost for latency and propose a multi-hop taxonomy function.

In Fig. 4(a) and (b), the taxonomy function is evaluated for MicaZ and Mica2 nodes, respectively. The taxonomy function is normalized for the maximum value of ARQ. It is clear from (46) that a higher value of $\mathcal{T}$ corresponds to higher efficiency. It can be observed from Fig. 4(a) that for the MicaZ nodes, the FEC codes outperform ARQ. Moreover, RS codes are less efficient compared to the BCH codes due to their higher energy consumption. Moreover, an optimal error correction capability, t, can be found for both BCH and RS codes that leverages the PER with energy consumption and latency. On the other hand, for Mica2 nodes, ARQ is more efficient than the FEC codes. This interesting result advocates that there is no clear winner for error control techniques in WSNs and their performance directly depends on the node hardware.

The reason behind the difference between MicaZ and Mica2 nodes can be explained as follows: In Fig. 4(c), the taxonomy function is re-evaluated for Mica2 without considering the energy consumption of neighbor nodes, E_{neigh}, given in (17). In this case, all the FEC codes except BCH (128,50,13) are more efficient than ARQ. The major differences between Mica2 and MicaZ nodes are the data rate of the transceivers and the modulation schemes. As shown in Table I, the time consumed for

transmitting a bit is 15 times higher for Mica2 than MicaZ. This corresponds to significant energy consumption for communication. Since the peak of the ARQ curve corresponds to no retransmissions, it is clear that the FEC codes consume more energy primarily due to the transmission of redundant bits. When the energy consumption of the neighbors are also considered, the energy consumption significantly increases. Moreover, FEC codes lead to smaller increase in expected hop length for Mica2 nodes than MicaZ nodes. As a result, for Mica2 nodes, the advantage of larger hop length provided by the FEC codes is outweighed by the increase in energy consumption of neighbor nodes. This favors ARQ for Mica2 nodes. It is also important to note that consideration of E_{neigh} is important to accurately assess the performance of ARQ and FEC.

B. Transmit Power Control

Another technique to exploit the error resiliency of FEC codes is to decrease the transmit power, P_t. In order to investigate the effect of transmit power, P_t, we consider three power levels, i.e., 0, -5, and -15 dBm supported by both Mica2 and MicaZ. Intuitively, decreasing transmit power can improve the energy efficiency of the FEC schemes, since less power is consumed for transmission of longer encoded packets. Although the receive power is fixed, since the interference range of a node decreases, the number of neighbors that consume idle energy also decreases. On the other hand, decreasing transmit power increases the number of hops. In Fig. 5(a), the energy consumption of BCH (128,50,13) and RS (15,9,3) are shown for three
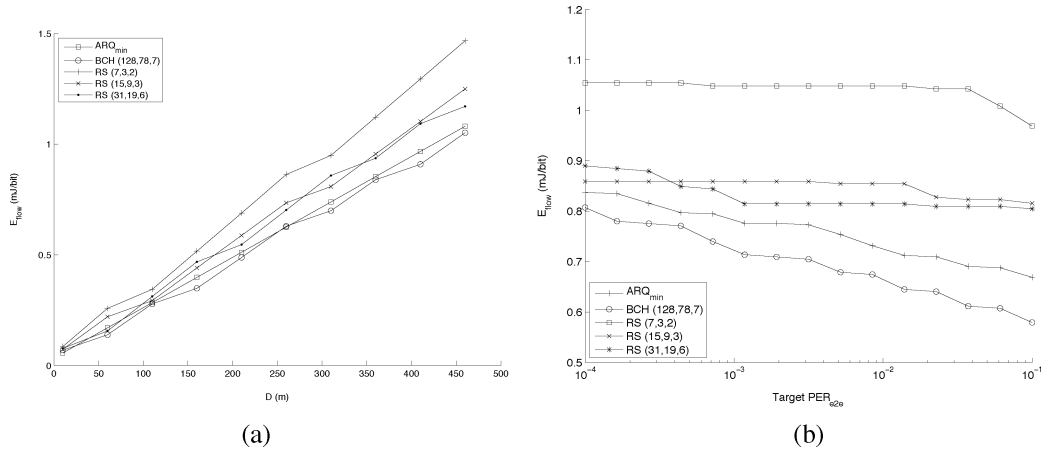
Fig. 6. Average energy consumption versus (a) end-to-end distance and (b) target end-to-end PER for MicaZ nodes.

different transmit power levels and ARQ at $P_t = 0$ dBm. Note that the decrease in transmit power decreases the end-to-end energy consumption for both BCH and RS codes, which outperform the ARQ scheme for lower transmit power levels.

While transmit power control provides energy efficiency for particular FEC codes, its drawback is shown in Fig. 5(b), where the end-to-end latency is shown. Contrary to the hop distance extension, since controlling transmit power has no effect in the time required for transmitting a packet, the end-to-end latency depends on the number of hops. Since transmit power control increases the number of hops, this technique introduces a significant increase in latency, which is a tradeoff for the FEC codes.

C. Effects of Network Conditions

In this section, we investigate the effects of end-to-end distance, D, the target PER, PER^*_{e2e}, and channel load on the performance of ARQ and FEC schemes. The end-to-end energy consumption per useful bit is shown in Fig. 6(a) as a function of the end-to-end distance, D, for MicaZ nodes. In this figure, the minimum ψ_{Th} is selected for each BCH and RS code such that $PER^*_{e2e} \leq 10^{-2}$ is satisfied.[5] Accordingly, BCH code with $t = 7$ results in energy consumption comparable to ARQ. In particular, ARQ is more energy efficient for end-to-end distances up to ~ 20 m, which corresponds to single hop communication. As expected, for single hop communication, the hop length extension capability of FEC codes cannot be exploited. For hop counts higher than these values, the BCH code consumes slightly less energy compared to ARQ. Furthermore, RS codes result in energy consumption that is higher than both ARQ and the BCH (128,78,7) code. Moreover, RS (7,3,2) code results in highest energy consumption since the energy resiliency provided by the low error correction capability ($t = 2$) does not overweigh the overhead because of redundant bit transmissions and decoding. For Mica2 nodes, ARQ is more energy efficient than both of the FEC codes irrespective of the end-to-end distance.

As explained before, the operating point of ψ_{Th} is determined according to the target PER of the WSN application. The effect of target PER is investigated in Fig. 6(b) for MicaZ nodes.

[5]For clarity, only BCH (128,78,7) code is shown with the three RS codes.

Similar to our observations above, when MicaZ architecture is considered, BCH code outperforms ARQ in terms of energy consumption. When the target PER is increased, the optimal value of ψ_{Th} is decreased, which improves the energy efficiency of FEC codes. As a result, the energy consumption of BCH (128,78,7) code is more favorable than ARQ. On the contrary, irrespective of the end-to-end PER requirement, RS codes always result in higher energy consumption than both ARQ and the BCH (128,78,7). Furthermore, there exist an optimal value for error correction capability for RS codes. As shown in Fig. 6(b), for small t, energy consumption is significantly high. Moreover, for target PER values below $PER_{e2e} < 0.006$, RS (15,9,3) outperforms other RS codes. On the other hand, if the target PER is relaxed, RS code with higher error correction capability is more energy efficient.

Finally, the effect of medium access control is shown in Fig. 7(a), where the x-axis shows the channel load λ, y-axis is the maximum normalized taxonomy, and the values are shown for BCH (128,78,7) and RS (15,9,3). The vulnerability of the contention-based MAC scheme under high traffic load as well as high density can be observed by increasing λ. The maximum normalized taxonomy value is found from the taxonomy function shown in Fig. 5, which is normalized according to the ARQ protocol with 10 retransmissions. Consequently, this value shows the maximum improvement in efficiency for both FEC schemes. It is clear that as the channel load increases, the collision rate increases, which leads to more number of retransmissions for each channel access attempt. This reduces the efficiency of each error control technique. However, as shown in Fig. 7(a), higher traffic load improves the normalized taxonomy for both BCH and RS codes. Since ARQ protocol provides error resiliency through retransmissions, each retransmission is susceptible to collisions when the channel load is high. Consequently, the effective traffic load λ_{net} shown in (21) increases further, resulting in lower efficiency compared to the FEC codes, which do not suffer from retransmissions. Furthermore, note that the traffic load λ is a function of both the packet generation rate and the density of the network. Consequently, as shown in Fig. 7(a), FEC codes are significantly more efficient than ARQ codes in WSN where the network density and the traffic rate is high.
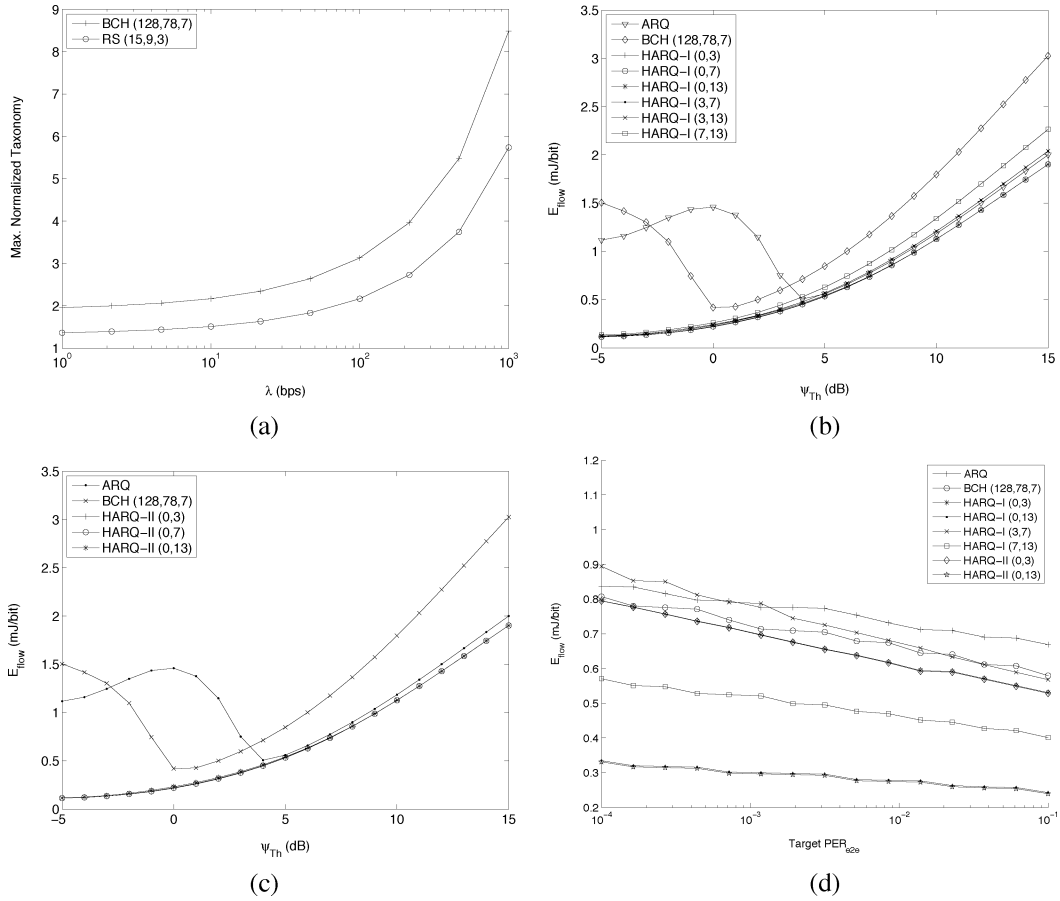
Fig. 7. (a) Maximum normalized taxonomy versus traffic load, λ. Average energy consumption versus ψ_{Th} for hybrid ARQ (b) Type I and (c) Type II and (d) average energy consumption versus target end-to-end PER (MicaZ).

D. Hybrid Error Control

Hybrid ARQ schemes exploit the advantages of both ARQ and FEC techniques. In this section, we compare the end-to-end energy consumption and the latency characteristics of these schemes with the ARQ scheme and the BCH (128,78,7), which is found to be the most energy-efficient FEC scheme in the previous sections.

The energy consumption of the type I and type II hybrid ARQ schemes are shown in Fig. 7(b) and (c), respectively, for MicaZ. An important result is that type II hybrid ARQ schemes are more energy efficient than both ARQ and FEC schemes. As shown in Fig. 7(c), the energy consumption of different HARQ-II schemes are similar for a given ψ_{Th} value. However, since the error resiliency of these protocols depend on the BCH code used, the operating point of these schemes differ based on the target PER. It is shown in Fig. 7(b) that the energy consumption of the HARQ-I scheme is dependent on the error correction code used in the first transmission. Consequently, HARQ-I (7,13) scheme results in slightly higher energy consumption for a given ψ_{Th} value.

The energy consumption curves in Fig. 7(b) and (c) as a function of the SNR threshold, ψ_{Th}, illustrate the effect of this threshold on the performance of these error control schemes. However, for a given end-to-end reliability require-ment, the operating point of ψ_{Th} is different for each scheme because of their different error resiliency. In Fig. 7(d), the end-to-end energy consumption is shown as a function of the target PER for MicaZ nodes. It can be observed that HARQ-II schemes outperform ARQ, FEC, as well as HARQ-I schemes. This is particularly appealing since the HARQ-II scheme is implemented through only a single BCH code. Hence, the implementation cost of the HARQ-II scheme in consideration is also low compared to the HARQ-I case, where two different encoding schemes needs to be implemented. Furthermore, the energy efficiency of HARQ-II schemes improve when more powerful FEC schemes are used.

E. Overview of Results

An overview of the energy and latency performance of the error control schemes that are considered in this paper is shown in Fig. 8 for MicaZ nodes. In the figures, the minimum end-to-end energy consumption and latency of ARQ, BCH, RS, HARQ-I, and HARQ-II schemes subject to an end-to-end PER target of 10^{-2} are shown as a function of their error correction capability. In particular, in Fig. 8(a) and (b), the minimum energy consumption and latency of these schemes are shown. Consistent with our previous observations, both type-I and type-II hybrid ARQ schemes outperform other error control schemes. Moreover, it can be observed that for both BCH and RS codes, an optimum error correction capability, t, value can be found to minimize the energy consumption and latency. The results reveal that type-I hybrid ARQ codes are inefficient in
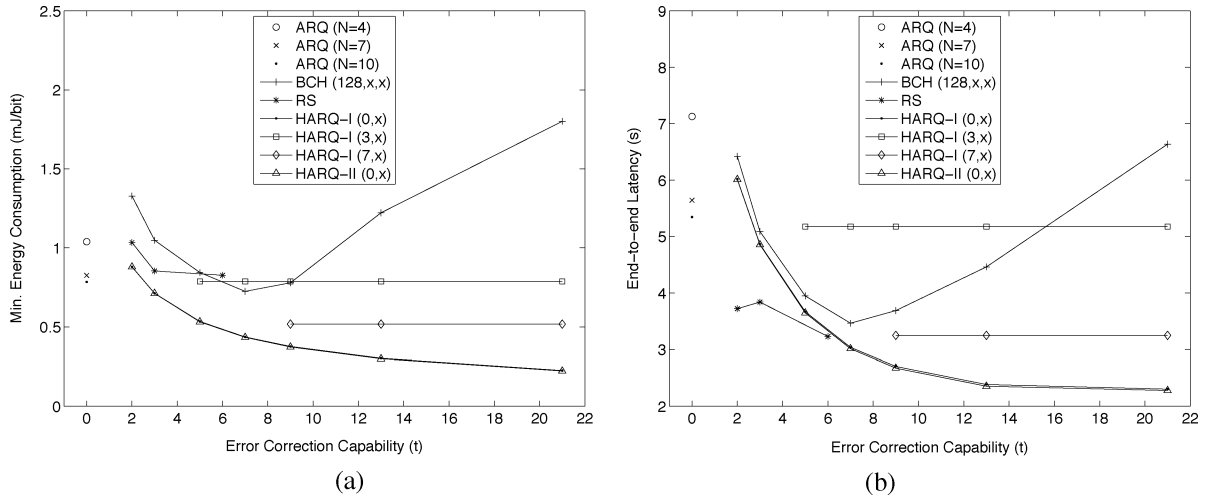
Fig. 8. (a) Minimum energy consumption versus error correction capability and (b) minimum end-to-end latency versus error correction capability for MicaZ.

TABLE II
OVERVIEW OF RESULTS

	Hop Length Ext.		Tx. Power Cont.	
	Energy	Latency	Energy	Latency
Mica2	HARQ I&II	HARQ I&II	BCH $(t \geq 1)$	ARQ
MicaZ	HARQ II (RS)	HARQ II	BCH $(t \geq 1)$	ARQ

terms of both energy consumption and latency. Type-II hybrid ARQ scheme is more energy efficient compared to ARQ, BCH, and RS codes. Furthermore, it can be observed from Fig. 8(b) that RS (31,19,6) code performs very close to the HARQ-II scheme in terms of end-to-end latency, which make both of these schemes a suitable candidate for real-time traffic.

VI. CONCLUSION

In this paper, a cross-layer analysis of error control schemes is presented. Forward error correction (FEC) coding improves the error resiliency by sending redundant bits through the wireless channel. It is shown that this improvement can be exploited by *transmit power control* or *hop length extension* through channel-aware cross-layer geographical routing protocols in WSNs. The results of our cross-layer analysis are summarized in Table II, where the efficient schemes are identified. Accordingly, hop length extension decreases both energy consumption and end-to-end latency for certain FEC codes when compared to ARQ. On the other hand, transmit power control can be exploited in situations where energy consumption is of paramount importance and can be traded off for end-to-end latency. In this paper, the effects of hybrid ARQ schemes are also investigated and a comprehensive comparison of these three error control schemes are presented. Moreover, it has been shown that the selection of suitable error control scheme depends on the physical architecture of the sensor nodes as well as the end-to-end distance and target PER. Furthermore, the advantages of FEC schemes in high density networks with high traffic rate are also highlighted. Finally, FEC and hybrid ARQ schemes are shown to significantly improve the end-to-end latency performance

of WSNs through hop length extension without hampering the energy efficiency and the end-to-end PER. This makes these schemes important candidates for delay sensitive traffic in WSNs when used in combination with retransmissions in hybrid ARQ schemes.

An important assumption in our derivations is that the encoding and decoding operations for the FEC schemes are performed in software. While this operation can lead to energy efficient operation as shown in evaluation results, the efficiency is limited by the CPU capacity of the hardware. Considering the potential advantages of incorporating FEC schemes into communication in WSNs as shown in this paper, hardware support for encoding and decoding operations is essential. Especially, the significant increase in efficiency of FEC schemes in high density network with high traffic load motivates novel hardware platforms in WSNs that can perform hardware encoding and decoding and can be used in multimedia applications.

REFERENCES

[1] I. F. Akyildiz, W. Su, Y. Sankarasubramaniam, and E. Cayirci, "Wireless sensor networks: A Survey," *Computer Networks J.*, vol. 38, no. 4, pp. 393–422, Mar. 2002.

[2] I. F. Akyildiz, M. C. Vuran, and O. B. Akan, "A cross-layer protocol for wireless sensor networks," in *Proc. Conf. Information Sciences and Systems (CISS'06)*, Princeton, NJ, Mar. 22–24, 2006.

[3] ATmega128 Datasheet. Atmel Corp. [Online]. Available: http://www.atmel.com

[4] G. Balakrishnan, M. Yang, Y. Jiang, and Y. Kim, "Performance analysis of error control codes for wireless sensor networks," in *Proc. Int. Conf. Information Technology (ITNG'07)*, 2007, pp. 876–879.

[5] Y. Barowski, S. Biaz, and P. Agrawal, "Towards the performance analysis of IEEE 802.11 in multi-hop ad-hoc networks," in *Proc. IEEE Wireless Communications and Networking Conf.*, Mar. 2005, vol. 1, pp. 100–106.

[6] E. R. Berlekamp, *Algebraic Coding Theory*. New York: McGraw-Hill, 1968.

[7] G. Bianchi, "Performance analysis of the IEEE 802.11 distributed coordination function," *IEEE J. Sel. Areas Commun.*, vol. 18, no. 3, pp. 535–547, Mar. 2000.

[8] J. Choi, J. So, and Y. Ko, "Numerical analysis of IEEE 802.11 broadcast scheme in multihop wireless ad hoc networks," in *Proc. Int. Conf. Information Networking*, 2005, pp. 1–10.

[9] Mica2 Datasheet. Crossbow Corp. [Online]. Available: http://www.xbow.com

[10] MicaZ Datasheet. Crossbow Corp. [Online]. Available: http://www.xbow.com

[11] H. Karvonen, Z. Shelby, and C. Pomalaza-Raez, "Coding for energy efficient wireless embedded networks," in *Proc. Int. Workshop on Wireless Ad-Hoc Networks*, Jun. 2004, pp. 300–304.

[12] M. A. Landolsi and W. E. Stark, "On the accuracy of Gaussian approximations in the error analysis of DS-CDMA with OQPSK modulation," *IEEE Trans. Commun.*, vol. 50, no. 12, pp. 2064–2071, Dec. 2002.

[13] S. Lin and D. J. Costello Jr., *Error Control Coding: Fundamentals and Applications*. Englewood Cliffs, NJ: Prentice-Hall, 1983.

[14] M. Luby, "LT- codes," in *Proc. 43rd Annual IEEE Symp. Foundations of Computer Science (STOC)*, 2002, pp. 271–280.

[15] Y. Sankarasubramaniam, I. F. Akyildiz, and S. W. McLaughlin, "Energy efficiency based packet size optimization in wireless sensor networks," in *Proc. IEEE Int. Workshop on Sensor Network Protocols and Applications*, 2003, pp. 1–8.

[16] V. Shnayder *et al.*, "Simulating the power consumption of large-scale sensor network applications," in *Proc. ACM SenSys'04*, Baltimore, MD, Nov. 2004.

[17] K. Schwieger, A. Kumar, and G. Fettweis, "On the impact of the physical layer on energy consumption in sensor networks," in *Proc. EWSN'05*, Feb. 2005, pp. 13–24.

[18] K. Seada, M. Zuniga, A. Helmy, and B. Krishnamachari, "Energy-efficient forwarding strategies for geographic routing in lossy wireless sensor networks," in *Proc. ACM Sensys'04*, Nov. 2004.

[19] A. Shokrollahi, "Raptor codes," *IEEE/ACM Trans. Networking, Special Issue on Networking and Information Theory*, vol. 52, no. 6, pp. 2551–2567, Jun. 2006.

[20] E. Shih *et al.*, "Physical layer driven protocol and algorithm design for energy-efficient wireless sensor networks," in *Proc. ACM Mobicom 2001*, Rome, Italy, Jul. 2001, pp. 272–286.

[21] P. Skraba, H. Aghajan, and A. Bahai, "Cross-layer optimization for high density sensor networks: Distributed passive routing decisions," in *Proc. Ad-Hoc Now'04*, Vancouver, Canada, Jul. 2004.

[22] S. Vural and E. Ekici, "Analysis of hop-distance relationship in spatially random sensor networks," in *Proc. ACM MobiHoc'05*, May 2005, pp. 320–331.

[23] M. C. Vuran and I. F. Akyildiz, "Cross-layer analysis of error control in wireless sensor networks," in *Proc. IEEE SECON'06*, Reston, VA, Sep. 2006.

[24] S. B. Wicker and M. J. Bartz, "Type-II hybrid-ARQ protocols using punctured MDS codes," *IEEE Trans. Commun.*, vol. 42, no. 2/3/4, pp. 1431–1440, Feb./Mar./Apr. 1994.

[25] M. Zorzi and R. Rao, "Geographic random forwarding (GeRaF) for ad hoc and sensor networks: Multihop performance," *IEEE Trans. Mobile Comput.*, vol. 2, no. 4, pp. 337–348, Dec. 2003.

[26] M. Zuniga and B. Krishnamachari, "Analyzing the transitional region in low power wireless links," in *Proc. IEEE SECON'04*, Oct. 2004, pp. 517–526.

Mehmet C. Vuran (M'98) received the B.Sc. degree in electrical and electronics engineering from Bilkent University, Ankara, Turkey, in 2002. He received the M.S. and Ph.D. degrees in electrical and computer engineering from the Broadband and Wireless Networking Laboratory, School of Electrical and Computer Engineering, Georgia Institute of Technology, Atlanta, in 2004 and 2007, respectively, under the guidance of Prof. Ian F. Akyildiz.

Currently, he is an Assistant Professor in the Department of Computer Science and Engineering at the University of Nebraska–Lincoln. His current research interests include cross-layer design and correlation-based communication for wireless sensor networks, underground sensor networks, cognitive radio networks, and deep space communication networks.

Dr. Vuran received the 2007 ECE Graduate Research Assistant Excellence Award from School of Electrical and Computer Engineering, Georgia Institute of Technology and the 2006 Researcher of the Year Award in Broadband and Wireless Networking Laboratory, School of Electrical and Computer Engineering, Georgia Institute of Technology. He serves as an Associate Editor of *Computer Networks Journal (Elsevier)* and *Journal of Sensors (Hindawi)*. He is also the guest editor of the *ACM MONET Journal* Special Issue on Wireless Heterogeneous Networks and *Next Generation Internet and Computer Communications Journal* (Elsevier) Special Issue on Cognitive Radio and Dynamic Spectrum Sharing Systems.

Ian F. Akyildiz (M'86–SM'89–F'96) received the B.S., M.S., and Ph.D. degrees in computer engineering from the University of Erlangen-Nuernberg, Germany, in 1978, 1981, and 1984, respectively.

Currently, he is the Ken Byers Distinguished Chair Professor with the School of Electrical and Computer Engineering, Georgia Institute of Technology, Atlanta, and Director of Broadband and Wireless Networking Laboratory. His current research interests are in sensor networks, next generation wireless networks, IPN Internet, wireless networks, and satellite networks.

Dr. Akyildiz is an Editor-in-Chief of *Computer Networks Journal (Elsevier)* as well as the founding Editor-in-Chief of the *AdHoc Network Journal (Elsevier)* and the *PHYCOM: Physical Communication Journal (Elsevier)*. He received the Don Federico Santa Maria Medal for his services to the Universidad of Federico Santa Maria, in 1986. From 1989 to 1998, he served as a National Lecturer for ACM and received the ACM Outstanding Distinguished Lecturer Award in 1994. He received the 1997 IEEE Leonard G. Abraham Prize Award (IEEE Communications Society) for his paper entitled "Multimedia Group Synchronization Protocols for Integrated Services Architectures" published in the IEEE JOURNAL OF SELECTED AREAS IN COMMUNICATIONS (JSAC) in January 1996. He received the 2002 IEEE Harry M. Goode Memorial Award (IEEE Computer Society) with the citation "for significant and pioneering contributions to advanced architectures and protocols for wireless and satellite networking". He received the 2003 IEEE Best Tutorial Award (IEEE Communication Society) for his paper entitled "A Survey on Sensor Networks," published in *IEEE Communications Magazine*, in August 2002. He also received the 2003 ACM Sigmobile Outstanding Contribution Award with the citation "for pioneering contributions in the area of mobility and resource management for wireless communication networks". He received the 2004 Georgia Tech Faculty Research Author Award for his "outstanding record of publications of papers between 1999–2003". He also received the 2005 Distinguished Faculty Achievement Award from School of Electrical and Computer Engineering, Georgia Tech. He has been a Fellow of the Association for Computing Machinery (ACM) since 1996.